Reflector Effects on the Performance of a Retrodirective Antenna Array

Vincent F. Fusco, Rajat Roy, and Shyam L. Karode

***Abstract*—This paper presents modeling strategies to determine the operating characteristics of a heterodyne phase-conjugate retrodirective Van Atta array in the presence of a plane reflector. The models used are based on physical and geometrical optics principles. Predictions of the operating characteristics of the array due to the close proximity of a plane metallic reflector are compared with experimental measurements. It is shown that provided the reflector is positioned at a distance greater than 1.25 times the separation distance between the transmitter and the retrodirective array its effect on the performance of the retrodirective array appears to be negligible.**

***Index Terms*—Antenna arrays, reflector antennas, retrodirectivity.**

I. Introduction

FIXED link wireless systems require the accurate pointing of high-gain antennas. Traditionally, with mobile systems, this is not possible and omnidirectional antennas with attendant reduction in signal strength are used. Previously, adaptive antenna techniques have been demonstrated to yield spatial frequency reuse [1]. These systems tend at present to be overly complex for a variety of lower performance mobile tracking applications, e.g., robotic vehicular. In general, in a retrodirective antenna array each array element is phased independently of every other. Hence, the array self corrects its phase response in order to track an incoming signal without a prior knowledge of the position of the incoming signal. This paper addresses the operational wireless situation where self-phased or retrodirective antenna array are used to automatically self-track a target via spatially selective antennas in the presence of a reflecting object placed close to the antenna. The operation of such a configuration with a reflector included is analyzed here for the first time using both geometrical and physical optics strategies.

II. Retrodirective Arrays

There are two basic types of planar retrodirective architectures namely the Van Atta [2] and the Pon [3] array. The retrodirective principle of operation, i.e., phase conjugating the received signal and returning it in the direction it came from, is achieved in the Van Atta case [2] by means of interchanging the signal received from one element of a multi-element structure with its symmetrically disposed equivalent element while maintaining equal time delays in either direction. In the Pon case [3], phase conjugation is achieved by mixing the spatially sampled incoming wavefront with a signal from a local oscillator running at twice the frequency and then returning it through the same element. The advantage of the Pon array over the Van Atta

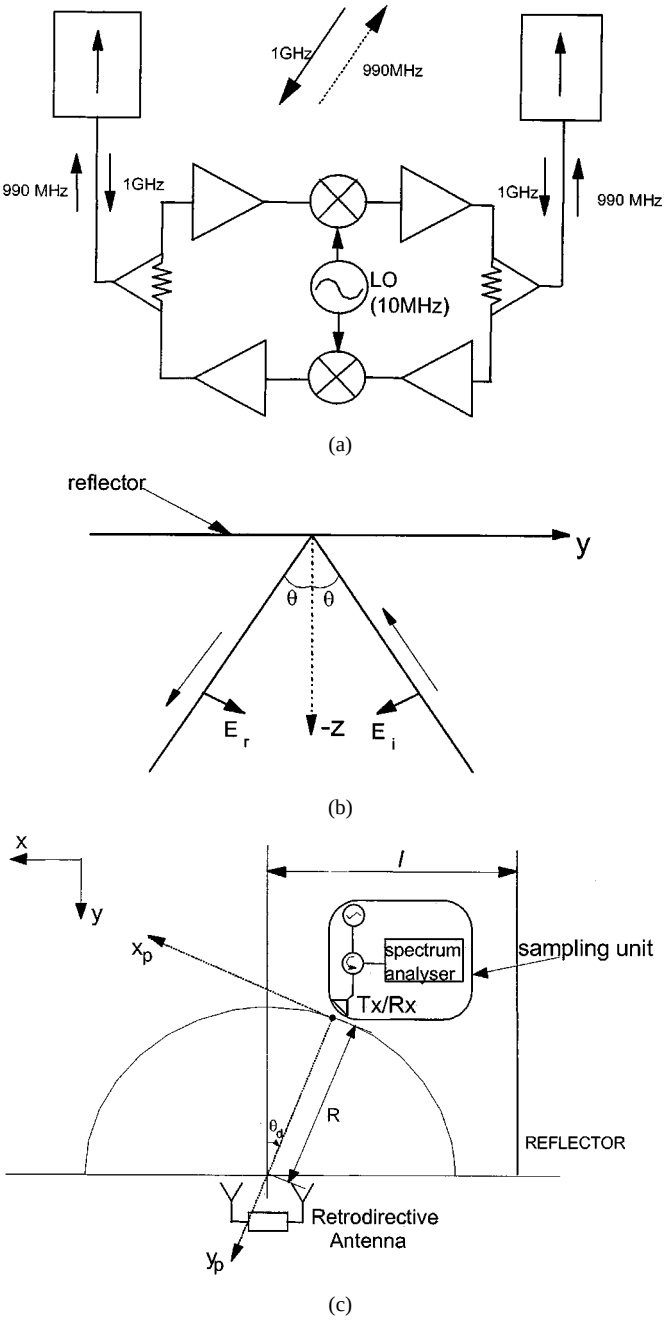

Fig. 1. Modeling and circuit definitions.

Manuscript received October 30, 1998; revised March 6, 2000. This work was supported by the British Commonwealth Commission, EPSRC, GR/L32866, and IRTU Grant ST175.

The authors are with the High-Frequency Electronics Laboratory, Department of Electrical and Electronic Engineering, The Queen's University of Belfast, Belfast BT9 5AH, U.K. (email: v.fusco@ee.qub.ac.uk).

Publisher Item Identifier S 0018-926X(00)05793-8.

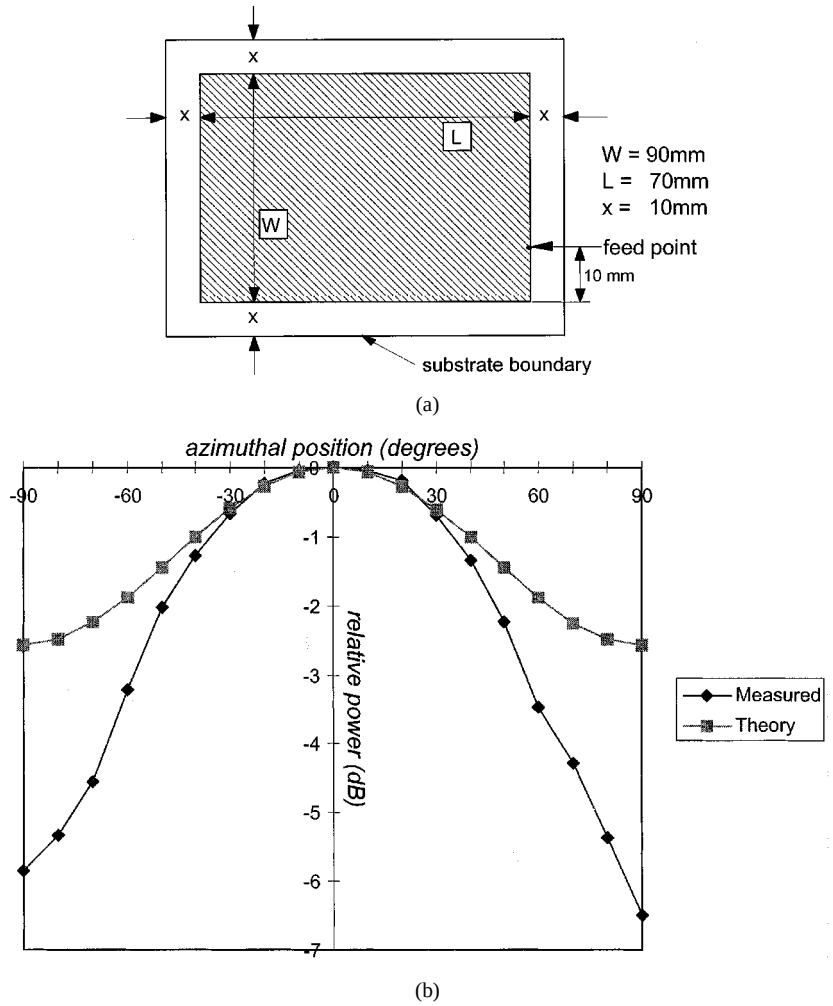

Fig. 2. Microstrip array sampling element.

array are that in the Pon structure array elements can be arbitrarily located on any kind of surface whereas in the Van Atta structure they must be located in a plane. The main disadvantage of the Pon array is that a local oscillator running at twice the frequency of the incoming signal is required. The type of retrodirective array tested here is a modification of the Van Atta array, which includes a bilateral offset frequency arrangement Fig. 1(a), a complete description of this architecture is given in [4]. In this paper, a study is undertaken with the purpose of showing the magnitude of the unwanted interference term introduced into the working of the array when it is operating close to a plane metallic reflector; such a situation could arise when the retrodirective array is operated in a mobile wireless environment as described in the introduction.

III. Multipath Reflections from Geometrical Optics

In the geometrical optics model, the reflector is taken as an infinite metal sheet as shown in the Fig. 1(b). $\boldsymbol{E}^i$ and $\boldsymbol{E}^r$ are the incident and the reflected field, respectively. The incident field is

$$E_z^i = -E_0 e^{-jk(z\cos\theta - y\sin\theta)}\sin\theta \tag{1}$$

$$E_y^i = -E_0 e^{-jk(z\cos\theta - y\sin\theta)}\cos\theta. \tag{2}$$

The condition to be satisfied at the boundary between the reflected and incident fields is

$$E_y^r = -E_y^i. \tag{3}$$

Also $\nabla.\boldsymbol{E}^i = 0$ and $\nabla.\boldsymbol{E}^r = 0$. The reflected ray that satisfies these is

$$E_z^r = -E_0 e^{jk(z\cos\theta + y\sin\theta)}\sin\theta \tag{4}$$

$$E_y^r = E_0 e^{jk(z\cos\theta + y\sin\theta)}\cos\theta. \tag{5}$$

In our geometrical optics calculations, we trace the path of such a ray from the transmit/receive unit in Fig. 1(c) to the retrodirective antenna. When at a certain position the ray from the transmit/receive unit falls behind the ground plane of the elements comprising the wavefront sampling array for the retrodirective array we have an abrupt termination of the ray. In this situation, its effect is lost in the overall computation. The same rule applies to the ray that misses the reflector. All other reflected rays impinge on the retrodirective array, which then operates as a secondary source.

The power retransmitted from the retrodirective array can be obtained by vectorially adding contributions from the reflected ray and the direct signal. The effective array factor is given as

$$E_{total} = e^{j(\omega t+\phi)}\left[A_0 + \sum_{1}^{m} A_m e^{j\Psi_m}\right] \tag{6}$$

where

$$A_m = a_m \sum_{-(N/2)}^{N/2} e^{j(2\pi x_i)((\sin\theta t_m/\lambda_t)-(\sin\theta r/\lambda_r))} \tag{7}$$

N number of elements in the array;
θ_t position of the transmitter measured from the broadside;
θ_r position of the receiver measured from the broadside;
x_i distance of ith element from array center;
A_0 array factor due to primary source;
m number of multipath signals present;
Ψ_m phase difference between primary and mth secondary signal;
A_m amplitude scaling factor;
θt_m position of the mth secondary source measured from the broadside of the retrodirective array;
λ_t wavelength of the transmit signal;
λ_r wavelength of the receive signal.

IV. Reflected Field Using Physical Optics Approximation

The scattered electric field E^s from a reflector [5] is

$$\boldsymbol{E}^s = \frac{1}{2\pi j\omega\varepsilon_0}\nabla\times\nabla\times\int\int\left(n\times\boldsymbol{H}^i\right)\frac{e^{-jk_0|r-r'|}}{|\boldsymbol{r}-\boldsymbol{r}'|}ds' \tag{8}$$

where an assumption has been made that there is no induced current in the shadow region of the reflector and the total magnetic field at the reflector is twice the incident field $\boldsymbol{H}^i$. This approximation works well for reflectors of dimensions of a few wavelengths [6]. In our problem, (8) will give corrections to the results obtained by pure geometrical optics. The incident electric field is given by [7] and is the radiation field of a microstrip patch antenna used in the transmit/receive unit to illuminate the retrodirective array here

$$E_\varphi = \frac{e^{-jk_0r}}{k_0r}\frac{\sin(k_0h\sin\theta\cos\varphi/2)}{k_0h\sin\theta\cos\varphi/2}\frac{\sin(k_0W\cos\theta/2)}{k_0W\cos\theta/2}\cdot\sin\theta\cos(k_0L\sin\theta\cos\varphi/2). \tag{9}$$

Some modifications to this expression are necessary off boresight in order to accommodate the finite ground plane used in the experimental setup. The coordinate system used for modeling is shown in Fig. 1(c).

We now present a detailed treatment of the coordinate transformation on (9) to make it suitable for evaluating the incident magnetic field $\boldsymbol{H}^i$ in (8). The patch coordinates x_p and y_p are as shown in Fig. 1(c) and a right-handed coordinate system is assumed throughout. The coordinate system, fixed at the center

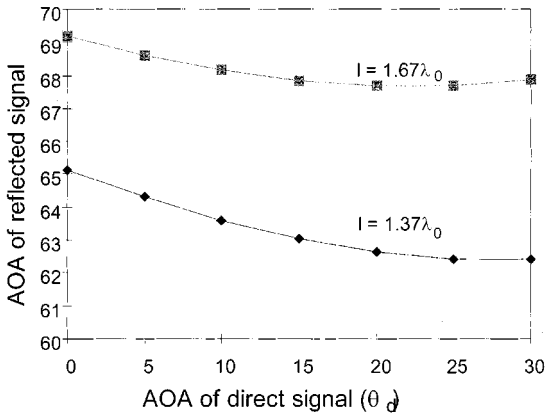

Fig. 3. Calculated AoA of the reflected signal with respect to the boresight of the retrodirective array.

of the retrodirective antenna, is also shown. The semi-circle in which the patch moves is of radius R and the inclination between the two coordinate systems is θ_d. The transformation between the two systems is

$$\begin{aligned} z &= z_p \\ x &= x_p\cos\theta_d + (y_p - R)\sin\theta_d \\ y &= -x_p\sin\theta_d + (y_p - R)\cos\theta_d \end{aligned} \tag{10}$$

The electric field given by (9) is first resolved into components parallel to x_p, y_p and z_p to give

$$\begin{aligned} E_{x_p} &= \frac{e^{-jk_0(x_p^2+y_p^2+z_p^2)^{0.5}}}{\left(x_p^2+y_p^2+z_p^2\right)^{0.5}}\frac{\sin\left(\dfrac{k_0hx_p}{2\left(x_p^2+y_p^2+z_p^2\right)^{0.5}}\right)}{\dfrac{k_0hx_p}{2\left(x_p^2+y_p^2+z_p^2\right)^{0.5}}} \\ &\quad\times\frac{\sin\left(\dfrac{k_0Wz_p}{2\left(x_p^2+y_p^2+z_p^2\right)^{0.5}}\right)}{\dfrac{k_0Wz_p}{2\left(x_p^2+y_p^2+z_p^2\right)^{0.5}}}\frac{y_p}{\left(x_p^2+y_p^2+z_p^2\right)^{0.5}} \\ &\quad\times\cos\left(\frac{k_0Lx_p}{2\left(x_p^2+y_p^2+z_p^2\right)^{0.5}}\right) \\ E_{y_p} &= -\frac{x_p}{y_p}E_{x_p} \\ E_{z_p} &= 0. \end{aligned} \tag{11}$$

These components of the field transform in exactly the same way as the coordinates

$$\begin{aligned} E_x &= E_{x_p}\cos\theta_d + E_{y_p}\sin\theta_d \\ E_y &= -E_{x_p}\sin\theta_d + E_{y_p}\cos\theta_d \\ E_z &= E_{z_p}. \end{aligned} \tag{12}$$

By successively applying transformations (10) and (11) to (12) we get an expression for the incident electric field in the x–y–z system. The incident magnetic field $\boldsymbol{H}^i$ of (8) is obtained from the expression for the radiation field

$$\boldsymbol{H}^i = (\boldsymbol{E}\times\boldsymbol{r})/\eta \tag{13}$$

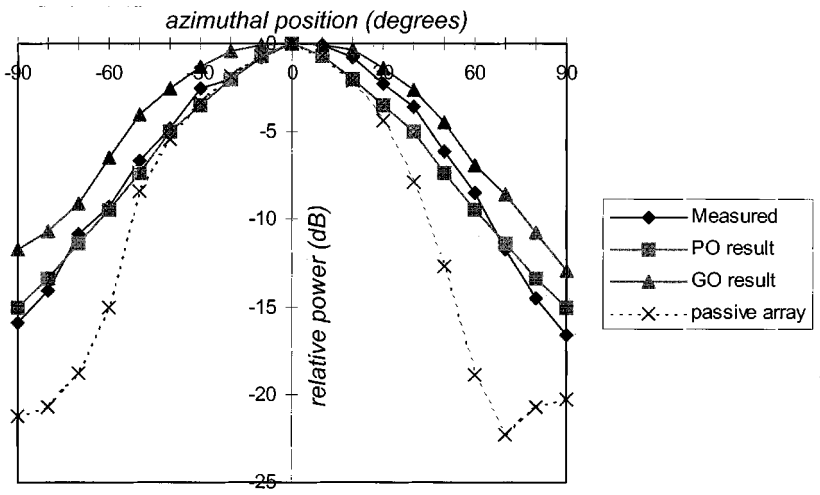

Fig. 4. Radiation patterns of the retrodirective antenna with no reflector present.

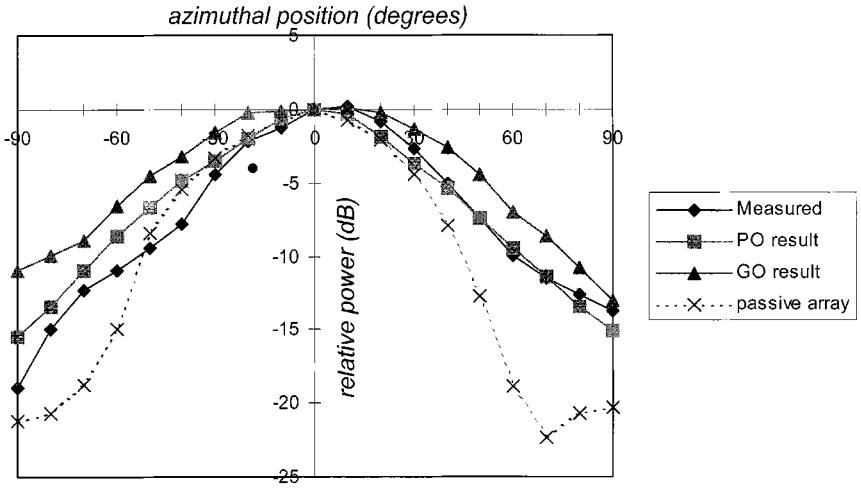

Fig. 5. Radiation patterns of the retrodirective antenna with reflector at $1.67\lambda_0$.

where $\boldsymbol{r}$ is the unit vector in the direction of propagation and η the free-space intrinsic impedance. The components of the scattered field by the reflector can be evaluated at the origin of Fig. 1(c), which is the location of the retrodirective antenna, however, as is necessary to simulate retrodirective antenna action we proceed as follows. The E_z^s component is the cross-polarization component, which is assumed not to excite the antenna. The scattered field at each of the elements of the retrodirective antenna are obtained by multiplying this field at the origin with

$$A_0 e^{(-jkdx_1/2(x_1^2+y_1^2+z_1^2)^{0.5})} \quad \text{or} \quad A_1 e^{(+jkdx_1/2(x_1^2+y_1^2+z_1^2)^{0.5})} \tag{14}$$

where the negative or positive signs in the exponential is taken for the left and the right microstrip patch, respectively, of the retrodirective antenna in Fig. 1(c). Here x_1, y_1 and z_1 are the coordinates of a point located on the plane reflector and d the interelement spacing of the array. Coefficients A_0 and A_1 are in general complex weights, which can be used to model any amplitude and phase distortions introduced by the amplifier, mixer, and connecting cables in Fig. 1(a). In our work they are both set equal to magnitude one and angle zero degrees. In the case of the retrodirective antenna [2], [3] when retransmitting the power back we refrain from carrying out the integral in (8), but we interchange the signs of the two exponentials above as they are phase conjugated according to (14) and for all elements ds' we sum up the field at the point in space where we place the receiver; this we call the reflected field. Similarly the power which comes out directly from the transmitting patch to the retrodirective antenna is also retransmitted back with a similar phase-conjugation procedure applied to the receiving patch; we call this the direct field. We neglect all scattering by the reflectors in the return path because the retrodirective antenna beam is more directed and in the case of the beam being focused toward the reflectors the receiving patch whose radiation pattern is concentrated into its forward half-space is unable to detect it.

The results of the physical optics model converged to the one obtained from geometrical optics when the reflector size was increased. For the infinite reflector of the geometrical optics algorithm we get a maximum scattered E field value, which is 28.5 dB below the direct field at the retrodirective antenna. For a reflector size of $2.33\lambda_0 \times 1.0\lambda_0$ the physical optics model predicts a maximum scattered power of -22.5 dBm when 0 dBm is radiated by the transmitter. However when the reflector

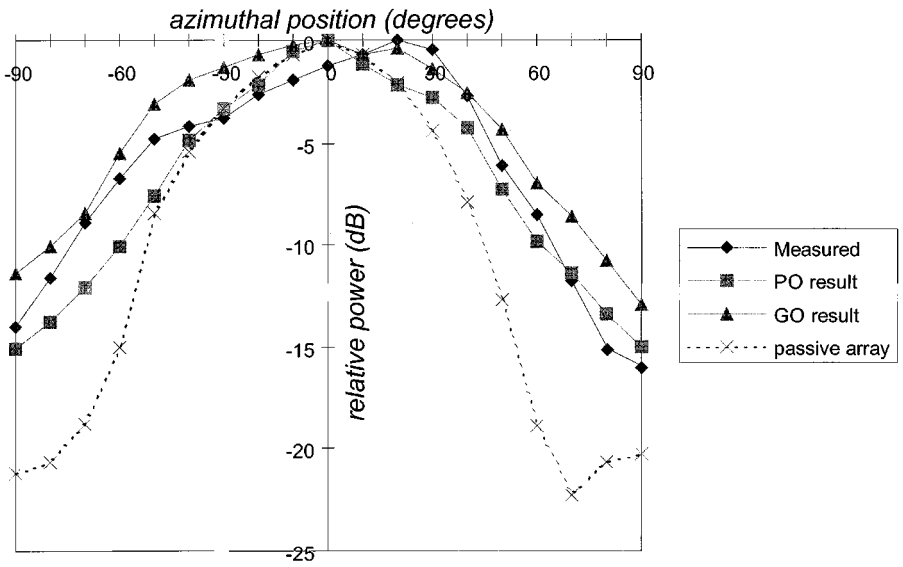

Fig. 6. Radiation patterns of the retrodirective antenna with reflector at $1.37\lambda_0$.

size is increased to $2.33\lambda_0 \times 1.67\lambda_0$ this value becomes -11.4 dBm which being very close to the value obtained from geometrical optics (-11.7 dBm) illustrates the convergence of the physical optics model to the geometrical optics model. It should be noted that it is difficult to verify these results experimentally as the fields coming directly from the transmitting patch to the retrodirective array are strong compared to $\boldsymbol{E}^s$ and cannot be suppressed for separate evaluation.

V. Estimation of Signal Levels at the Retrodirective Array

The Lorentz reciprocity theorem [5] when applied to a source free region states

$$\oint\!\!\!\!\!\!\int_{\mathrm{s}} (\boldsymbol{E}_1 \times \boldsymbol{H}_2 - \boldsymbol{E}_2 \times \boldsymbol{H}_1) \,.\boldsymbol{ds} = 0 \tag{15}$$

where S is the surface enclosing that region. We use this to obtain an estimate of power level received at one of the patches of the retrodirective array. Since the power flows into the patch antennas through a coaxial cable the region whose surface is S excludes all metallic surfaces and includes the dielectric region between the inner and outer conductor of the cable the dielectric patch substrate and an infinite sphere surrounding the receiver. The only contributions to the integral comes from the surface of the infinite sphere and the cross-sectional area of the cable. The subscripts 1 and 2 for the fields in (15) can be considered to stand for the fields of the antenna in the transmitting and the receiving modes respectively. For the cross section of the cable

$$\boldsymbol{E}_1 = \boldsymbol{A}e^{-jkz} \quad \text{and} \quad \boldsymbol{H}_1 = \frac{1}{Z_0}\,\hat{\boldsymbol{z}} \times \boldsymbol{A}e^{-jkz} \tag{16}$$

where

Z_0 characteristic impedance of the coaxial transmission line;

z coordinate along which the wave travels within it;

k propagation constant which is the free-space propagation constant k_0 multiplied by the square root of the dielectric constant of the material in the line.

In the transmitting mode, the power delivered to the antenna by the cable is

$$P_0 = \frac{1}{2}\,\mathrm{Re} \iint_{\mathrm{cross-section}} \boldsymbol{E}_1 \times \boldsymbol{H}_1^* \,.\boldsymbol{ds} = \frac{\boldsymbol{A}.\boldsymbol{A}^*}{2Z_0} = \frac{A^2}{2Z_0}. \tag{17}$$

In the receiving mode

$$\boldsymbol{E}_2 = \boldsymbol{B}e^{+jkz} \quad \text{and} \quad \boldsymbol{H}_2 = \frac{-1}{Z_0}\,\hat{\boldsymbol{z}} \times \boldsymbol{B}e^{+jkz}. \tag{18}$$

Therefore

$$\iint_{\mathrm{cross-section}} (\boldsymbol{E}_1 \times \boldsymbol{H}_2 - \boldsymbol{E}_2 \times \boldsymbol{H}_1) \,.\boldsymbol{ds} = -\frac{2\boldsymbol{A}.\boldsymbol{B}}{Z_0} = \frac{-2AB}{Z_0} = -4P_0\,\frac{B}{A}. \tag{19}$$

For the outer sphere, in the in the transmitting mode at large radius r

$$\boldsymbol{E}_1 = \frac{e^{-jk_0 r}}{k_0 r}\boldsymbol{e}(\theta, \phi) \quad \text{and} \quad \boldsymbol{H}_1 = \frac{1}{\eta}\,\hat{\boldsymbol{r}} \times \frac{e^{-jk_0 r}}{k_0 r}\,\boldsymbol{e}(\theta, \phi) \tag{20}$$

where η is free-space wave impedance. In the receiving mode the field consists of the incoming wave in the direction $-\hat{\boldsymbol{i}}$ and a scattered field of the type given by (20); that is

$$\boldsymbol{E}_2 = e^{jk_0 r\hat{\boldsymbol{r}}.\hat{\boldsymbol{i}}}\boldsymbol{e}_i + \frac{e^{-jk_0 r}}{k_0 r}\,\boldsymbol{e}_s(\theta, \phi)$$

and

$$\boldsymbol{H}_2 = \frac{1}{\eta}\left[-\hat{\boldsymbol{i}} \times e^{jk_0 r\hat{\boldsymbol{r}}.\hat{\boldsymbol{i}}}\,\boldsymbol{e}_i + \hat{\boldsymbol{r}} \times \frac{e^{-jk_0 r}}{k_0 r}\,\boldsymbol{e}_s(\theta, \phi)\right] \tag{21}$$

and so

$$\iint_{\text{surfaceoflargesphere}} (\boldsymbol{E}_1 \times \boldsymbol{H}_2 - \boldsymbol{E}_2 \times \boldsymbol{H}_1) \,.\boldsymbol{ds}$$
$$= \frac{e^{-jk_0 r}}{\eta k_0 r} \int_{-\pi/2}^{\pi/2} \int_{-\pi}^{\pi} \left[\boldsymbol{e}(\theta, \phi) \times \left\{-\hat{\boldsymbol{i}} \times \hat{\boldsymbol{e}}_i\right\} - \boldsymbol{e}_i \times \{\hat{\boldsymbol{r}} \times \boldsymbol{e}(\theta, \phi)\}\right] .(-\hat{\boldsymbol{r}})\, e^{jk_0 r \hat{\boldsymbol{r}}.\hat{\boldsymbol{i}}} r^2 \sin\theta \, d\phi \, d\theta - \frac{e^{-j2k_0 r}}{\eta (k_0 r)^2} \int_{-\pi/2}^{\pi/2} \int_{-\pi}^{\pi} [\boldsymbol{e}(\theta, \phi) \times \{\hat{\boldsymbol{r}} \times \hat{\boldsymbol{e}}_s(\theta, \phi)\} - \boldsymbol{e}_s(\theta, \phi) \times \{\hat{\boldsymbol{r}} \times \boldsymbol{e}(\theta, \phi)\}] (-\hat{\boldsymbol{r}}) r^2 \sin\theta \, d\phi \, d\theta. \quad (22)$$

The second of these integrals identically vanishes and the first can be evaluated computationally or by the method of stationary phase for large values of $k_0 r$ using the identity [8]

$$\iint_D f(x, y) e^{jKg(x,y)} \, dx \, dy = \frac{j2\pi f(x_0, y_0)\, e^{jKg(x_0, y_0)}}{K\sqrt{g_{xx} g_{yy} - g_{xy}^2}} \quad (23)$$

where $g_{xx} = (\partial^2 g / \partial x^2)$, etc., at a point where $g(x, y)$ is stationary (x_0, y_0) in the case when K is very large. Thus, we get

$$\iint_{\text{surfaceoflargesphere}} (\boldsymbol{E}_1 \times \boldsymbol{H}_2 - \boldsymbol{E}_2 \times \boldsymbol{H}_1) \,.\boldsymbol{ds} = \frac{j\lambda^2}{\eta\pi} (\boldsymbol{e}_i \,.\boldsymbol{e}(\theta, \phi)). \quad (24)$$

One obtains from (15), (19), and (24) the received power, which is

$$p_{\text{rec}} = \frac{|B|^2}{2Z_0} = \frac{\lambda^4 |\boldsymbol{e}_i.\boldsymbol{e}(\theta, \phi)|^2}{16\pi^2 P_0 \eta^2}. \quad (25)$$

When the polarization of $\boldsymbol{e}_i$ and $\boldsymbol{e}(\theta, \phi)$ are the same the power density (Poynting Vector) of the incoming wave which is $|\boldsymbol{e}_i|^2/(2\eta)$ gives the aperture area as

$$Ap \text{ area} = \frac{P_{\text{rec}}}{|\boldsymbol{e}_i|^2/(2\eta)} = \frac{\lambda^4 |\boldsymbol{e}(\theta, \phi)|^2}{8\pi^2 P_0 \eta}. \quad (26)$$

Now, if the total power radiated by the transmitting antenna is 20 dBm and if it radiates according to (9) with an overall multiplicative amplitude E_0, then we have for an aperture efficiency of 100%

$$.1 = \frac{E_0^2}{2\eta k_0^2} \int_0^{2\pi} \int_0^{\pi/2} \left[\frac{\sin(k_0 h \sin\theta \cos\varphi/2)}{k_0 h \sin\theta \cos\varphi/2} \times \frac{\sin(k_0 W \cos\theta/2)}{k_0 W \cos\theta/2} \sin\theta \cos(k_0 L \sin\theta \cos\varphi/2)\right]^2 . \sin\theta \, d\theta \, d\phi. \quad (27)$$

Thus, $E_0 = 101.92$ V/m, which gives the total power density (Poynting Vector S_r) at the retro-trans/receiver

$$S_r = \frac{E_0^2}{2\eta k_0^2 r^2} = .231 \text{ W/m}^2. \quad (28)$$

If we have a similar antenna at the receiver then $|\boldsymbol{e}(\theta, \phi)|^2$ of (26) in the direction of the boresight is just E_0^2 and this divided by $2P_0\eta 4\pi^2/\lambda^2$ is just one upon the integral in (27) above. Thus, the aperture area of the retrotrans/receiver patch is obtained as shown in (28a), shown at the bottom of the page. From this and (28) (by multiplying the two) the maximum received power at the retrotrans/receiver is obtained as 8.1 dBm. At other angles from the array bore-sight the power will reduce according to the angular distribution of (9). From direct application of the path equation this equates to patch antenna gain of approximately 6 dB.

VI. Results and Discussion

The retrodirective antenna in the case of our study is made up of two patch elements designed to operate at a frequency of 1 GHz, their dimensions are given in Fig. 2(a). The separation between the two elements comprising the array is half a wavelength at 1 GHz. The antenna used in the transmit/receive unit as shown in Fig. 1 is of identical type to that used in the retrodirective array, all patches are constructed on FR4 substrate $\varepsilon_r = 4.55$, $h = 1.5$ mm. At the receive frequency of 990 MHz the antenna VSWR is 1.37 and at the antenna transmit frequency of 1 GHz it is 1.08. Due to the small size of the ground plane in Fig. 2(a), the measured radiation field patterns are used to shape the theoretical patch responses given by (9) prior to their use in the physical optics model [Fig. 2(b)]. In all cases, the measured cross-polarization response for the patch antennas used was less than -18 dB. To study the multipath effects the expressions in (6), (8) were evaluated for various values of l, the distance to the plane reflector, as defined in Fig. 1(c). The radius of the semicircle shown in the same figure is $1.23\lambda_0$ (near field distance is $1.12\lambda_0$). This geometric distribution was selected so as to form

$$Ap \text{ area} = \frac{\lambda^2}{\displaystyle\int_0^{2\pi} \int_0^{\pi/2} \left[\frac{\sin(k_0 h \sin\theta \cos\varphi/2)}{k_0 h \sin\theta \cos\varphi/2} \frac{\sin(k_0 W \cos\theta/2)}{k_0 W \cos\theta/2} \sin\theta \cos(k_0 L \sin\theta \cos\varphi/2)\right]^2 \sin\theta \, d\theta \, d\phi} = .028 \text{ m}^2 \quad (28a)$$

a worst-case scenario whereby the reflected ray could be made to have the maximum possible effect on the operating characteristics of the retrodirective array, i.e., E^s would be maximum. In addition the selected disposition between the transmit/receive unit and the retrodirective array acts always to keep the measurement arc obtained by moving the transmit/receive to the left of the reflector in Fig. 1(c), thus, no shadowing of this unit will occur. The dimensions of the reflector were chosen to be $1.67\lambda_0$ in the z-direction and $2.33\lambda_0$ in the y-direction [the edge which is visible in Fig. 1(c) was $2.33\lambda_0$]. The reflector is placed symmetrically with respect to the cross-sectional plane in which the figure is drawn when the plane perpendicular to this plane is considered. The transmit/receive unit consisting of a single microstrip patch element was moved along the semicircle as shown in Fig. 1(c). This patch has its boresight fixed in the direction of the radial line, R, Fig. 1(c), joining it and the retrodirective antenna along the radius of the semicircle forming the measurement arc.

We now present the results of two key experiments: one is for the reflector placed at a distance of $1.37\lambda_0$ from the direct line of the sight between the transmit/receive unit and the retrodirective array and the other at $1.67\lambda_0$. Fig. 3 shows how for each of these reflector locations the angle of arrival of the reflector signal measured with respect to the boresight of the retrodirective antenna varies. In each set, approximately a 2° variation of the angle of arrival (AoA) is expected as the transmit/receive unit is moved along its measurement arc. Here, the value of θ_d is restricted to be 30° since at values greater than this the microstrip patch antenna used in the transmit/receive unit will obstinately have its ground plane facing toward the reflector.

In Fig. 4, without the presence of a reflector, we would expect the results for the geometrical, physical optics models, and for the experimental results to be convergent. Functionally, this is seen to be indeed the situation with the physical optics result matching almost exactly the measured response of the antenna. The geometrical optics result is typically about 1–2 dB higher than the measured response over the measurement range. This is due to the infinite reflector assumption in-built in the geometrical optics theory returning an over large reflected signal. It can also be seen that above $+30$ and below -50°, the response of the passive array is inferior to that of its retrodirective counterpart, by as much as 7 dB. That is, comparison with the response of a passive two element array constituted using the same microstrip patch antennas as used in the retrodirective array shows that retrodirective action is indeed occurring since the azimuthal response of the retrodirective antenna is flatter than its equivalent passive counterpart.

In Fig. 5 with the reflector placed at $l = 1.67\lambda_0$ best agreement occurs between the physical optics model and the measured result, with the geometrical optics model providing overestimates for the same reasons as before of 1–2 dB in the measured azimuthal plane.

In Fig. 6, with the reflector brought closer to the nominal array boresight $l = 1.37\lambda_0$ on the nonreflector side the geometrical optics model again provides an overly optimistic estimate of the azimuthal response of the array. It should be noted that for the no reflector case the measured 5-dB beamwidth is approximately $\pm 40^\circ$, while, with the reflector placed at $l = 1.37\lambda_0$, the 5 dB beamwidth has increased to $\pm 50^\circ$. This suggests that as an asymmetrically disposed reflector is brought closer to the nominal boresight direction of the system, the presence of the reflector tends to flatten the response of the retrodirective array.

This is most probably due to the stronger reflections from the more closely spaced reflector causing the retrodirective array to respond to this reflection by forming a secondary beam in the direction of arrival of the reflector signal [9], while specular reflection causes a complementary response in the negative azimuthal sector. Here, the measured and modeled responses peaks at $+20^\circ$, which corresponds to the angle of arrival expected from the geometrical considerations from the stated geometry. From Fig. 4, the much weaker reflected signal should arrive at about $+63^\circ$, but its individual effect is masked by the strength of the direct signal, the ratio between them being 28 dB as already stated.

Various measurements and simulations leads to the conclusion that when the ratio R/l [R, l defined in Fig. 1(c)] is greater than 1.25 then the effect of the plane reflector can be ignored since the secondary signal caused by reflection has little effect when compared to the main signal due to the ratio of their relative signal strengths, typically this ratio is around -30 dB. The geometrical optics results are always valid for very large planar reflectors, whereas physical optics gives some corrections to these results for finite size reflectors with or without small deviations from the shape of a plane. At small distances (into the far field) from the signal source a finite reflector subtends a large solid angle at the source and, hence, appears to be more like an infinite reflector. Here the correction of physical optics over the geometrical optics results due to the finiteness of the object will not be very great. However, the results for both these approximations will tend to deviate from measurement because the physical optics assumption stated in Section IV above that the total tangential magnetic field based on geometrical optics is twice that of the incident field will start breaking down in this region. Hence, we start getting deviations in Fig. 6 of both the predicted values from the experimental values (the peak of GO and PO coincides although different from that of experiment). At large values of l for moderately sized reflectors the corrections given by the physical optics model will be adequate and, hence, we have the close resemblance of this result with that of measurement in Fig. 5. If one is looking for very accurate results for all values of l a more rigorous numerical code based on for example the method of moments or the finite-element method which take into account the finite size of the patch ground plane will be necessary.

VII. Conclusion

It has been shown that the presence of a plane reflector of size $1.67\lambda_0 \times 2.33\lambda_0$ approximates to within 0.3 dBm the same amount of scattered electric field as a reflector of infinite size. Further when this reflector is brought into the proximity of a retrodirective array it has the effect of broadening the retrodirective array response due to both specular and secondary retrodirective beam formation. When the ratio of the separation between the excitation source and the retrodirective array R and distance to the reflector l is made greater than 1.25, then the

reflector appears to have little discernible influence on the performance of the retrodirective array.

An application of the system studied can be found in real life mobile wireless structures where the presence of a large reflector causing multipath effects roaming near to about 1.25 times the distance between the transmitter and the retrotrans/receiver is always possible. One need not worry about the actual distances in wavelengths we have used in this study in order to make the measurement feasible in the laboratory environment because the strength of the received signals is dependent inversely on the square of the distance between all elements for a fixed wavelength. Therefore, if the distances between the transmitter, retrotrans/receiver and the reflector together with the reflector size are proportionally scaled up by any given factor, the above conclusion we made always holds. However, one needs to pay more attention to the fact that whether the size of the reflector which we have used in our measurement system and the computer simulations we have made using physical optics will be sufficient to conclude that the behavior of an infinite reflector placed at these same distances will be similar. We tend to answer this in the affirmative since the geometrical optics calculations are valid for only infinite reflectors and the results calculated by this method using Fig. 6 $(l/R = 1.11)$ show a deviation to within about 1.5 dB from the measured data in Fig. 4 (without the reflector) near the peak response.

ACKNOWLEDGMENT

The authors would like to thank the referees of this paperfor their useful comments.

REFERENCES

[1] P. Zetterberg and B. Ottersen, "The spectral efficiency of a base station antenna array system for spatially selective transmission," in *Proc. IEEE Veh. Technol. Conf. (UTC)*, Stockholm, Sweden, June 1994, pp. 1517–1521.

[2] L. C. Van Atta, "Electromagnetic Reflector," US Patent 2 908 002, 1959.

[3] C. Y. Pon, "Retrodirective array using the heterodyne technique," *IEEE Trans. Antennas Propagat.*, vol. AP-12, pp. 176–180, Mar. 1964.

[4] S. L. Karode and V. F. Fusco, "Active retrodirective antenna arrays for mobile communication applications," in *Colloquium Low-Cost Antenna Technol.*, London, U.K., 1998, pp. 9/1–9/5.

[5] R. F. Harrington, *Time Harmonic Electro-magnetic Waves*. New York: McGraw Hill, 1960.

[6] R. E. Collin and F. J. Zucker, Eds., *Antenna Theory—Part 2*: McGraw Hill, 1969.

[7] I. J. Bahl and P. Bhartia, *Microstrip Antennas*. Norwood, MA: Artech House, 1980.

[8] R. H. Clarke and J. Brown, *Diffraction Theory and Antennas*. Chichester, U.K.: Ellis Horwood, 1980.

[9] C. C. Cutler, R. Kompfner, and L. C. Tillotson, "A self steering array repeater," *Bell Syst. Tech. J.*, pp. 2013–2032, 1963.

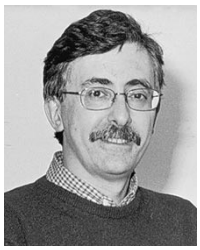

Vincent F. Fusco received the B.Sc. and Ph.D. (both first class honors) from Queens University of Belfast in 1979 and 1982, respectively.

He was a Research Engineer on short-range radar and radio telemetry systems and is currently a Professor of high-frequency electronic engineering in the School of Electrical Engineering, The Queen's University of Belfast, Ireland, U.K., where he is Head of the High-Frequency Research Group and Associate Dean of Research for Engineering. He has acted as a Consultant to government and international companies. His current research interests include nonlinear microwave circuit design, active antenna design and concurrent techniques for electromagnetic field problems.

He is a member of Institute of Electrical Engineers Professional Group E11 and various URSI committees. In 1996 he was awarded the NI Engineering Federation Trophy for exemplary industrially related research.

Rajat Roy received the Bachelor of Technology and the M.S. degrees from the Indian Institute of Technology, Kharagpur, India, in 1983 and 1984, respectively, and the Ph.D. degree from the University of Bombay, India, in 1996.

He was subsequently employed as a Scientific Officer at the Society for Applied Microwave Electronics Research (SAMEER), Indian Institute of Technology (IIT) Campus, Mumbai, India, where he was engaged in the design of microwave subsystems, components, and antennas. He was a Postdoctoral Researcher at The Queen's University of Belfast, Ireland, U.K., from 1997 to 1999. His principle areas of interest are antenna design and numerical electromagnetic techniques.

Shyam L. Karode received the primary degree from Marathwada University, Aurangabad, India, and the Ph.D. degree from The Queen's University of Belfast, Ireland, U.K., in 1998.

He carried out his postgraduate work at the Indian Institute of Technology, Kharagpur, India. From 1989 to 1995 he worked as a Scientific Officer at SAMEER, Center for Microwaves, Bombay, India, where he was engaged in various aspects of radar technology and industrial microwave heating. In 1995 he joined the High-Frequency Research Group, The Queen's University of Belfast. He is currently with INOTEK, Ltd., Sittingbourne, Kent, U.K. His current interests are in planar antenna and retrodirective array techniques for mobile communications.